Available online at www.sciencedirect.com

SCIENCE DIRECT®

Journal of Catalysis 225 (2004) 316–326

JOURNAL OF CATALYSIS

www.elsevier.com/locate/jcat

Increasing the basicity and catalytic activity of hydrotalcites by different synthesis procedures

M.J. Climent, A. Corma,* S. Iborra, K. Epping, and A. Velty

Instituto de Tecnología Química, UPV-CSIC, Universidad Politécnica de Valencia, Avd de los Naranjos s/n, 46022 Valencia, Spain

Received 8 March 2004; revised 13 April 2004; accepted 17 April 2004

Abstract

Hydrotalcites have been synthesized by three different procedures: conventional precipitation-aging, aging under microwave irradiation, and sonication during the coprecipitation step. The synthesis procedure has an effect on the crystal size and textural properties of the hydrotalcite (HT) and the Al_2O_3–MgO mixed oxides formed upon calcination. HT samples prepared under sonication at 298 K are formed by dispersed and homogenous particles of 80-nm average particle size. They also produce upon calcinations the mixed oxides with the largest surface area ($\sim 300\ m^2\ g^{-1}$). This method of preparation increases not only the surface area but also the number of defects in the solid, leading to sites of higher basicity. This was determined by means of catalytic reactions such as Knoevenagel and aldol condensations which demand basic sites of different strengths.

Hydrotalcites were regenerated from mixed oxides by hydration while giving Brönsted basic sites. Samples originally prepared by sonication present smaller crystallite size and have a larger number of accessible active sites. With these samples acetone/citral condensations with 96 and 99% conversion and selectivity, respectively, are achieved in a 15-min reaction time.

Keywords: Synthesis of hydrotalcites by sonication; Synthesis of hydrotalcites by microwave irradiation; Small crystal hydrotalcite; High surface area hydrotalcite

1. Introduction

Hydrotalcite-like compounds belong to a class of anionic clay minerals also known as layered double hydroxides (LDHs). They have the general molecular formula ${M_x}^{2+}{M_y}^{3+}(OH)_{2(x+y)}{A_{y/n}}^{-n} \cdot mH_2O$, where M^{2+} and M^{3+} are a divalent and a trivalent metal ions, respectively, and A^{-n} is an intercalated anion. Structurally, they are formed by brucite-like ($Mg(OH)_2$) sheets where isomorphous substitution of Mg^{2+} by a trivalent cation like Al^{3+} occurs. The positive charge of the layer is compensated by anions, which occupy the interlayer space along with water molecules [1]. The Al/Mg hydroxycarbonate LDH corresponds to the naturally occurring hydrotalcite mineral. Conventionally, these compounds are synthesized by coprecipitation, wherein metal nitrates and precipitants are added slowly and simultaneously at a fixed pH under stirring, followed by a long (about 1 day) ageing time and/or hydrothermal treatment in order to improve the crystallinity. The conditions of synthesis, i.e., temperature, pH, and metal composition, have been extensively studied [1–5]. By controlled thermal decomposition, LDHs are converted into mixed oxides, which possess homogeneous interdispersion of the elements, high specific surface areas, and, the most important, strong basic properties. The chemical composition of the hydrotalcites (the nature and amount of structural cations and compensating anions) is the main parameter that allows fine tuning of the basic strength. Nevertheless, for a particular chemical composition, the method of synthesis, i.e., temperature, solution pH, and ageing time of the gels, has a strong influence on the final basicity of the mixed oxides [1,6,7].

Microwave irradiation has been applied for the rapid synthesis of inorganic solids and organic synthetic reactions [8]. Pioneering work by Komarneni et al. [9–11] showed that microwave irradiation under hydrothermal conditions leads to very rapid synthesis of anhydrous ceramic oxides and

---

* Corresponding author. Fax: +34 96 387 7809.
E-mail address: acorma@itq.upv.es (A. Corma).

0021-9517/$ – see front matter © 2004 Elsevier Inc. All rights reserved.
doi:10.1016/j.jcat.2004.04.027

hydroxylated phases including hydrotalcites. Other authors have reported a crystallization rate enhancement of LDHs using microwaves [12,13]. More specifically, in the case of Mg/Al LDHs, Fetter et al. [14] have found that microwave irradiation of the coprecipitated gel allows well-crystallized and pure hydrotalcite-like phases to be obtained, and the ageing time can be reduced from 18–24 h to 2–10 min. Moreover, these authors have found that hydrotalcites obtained by this method present smaller crystallite sizes and higher specific surface areas than conventional samples, synthesized aging of the gels at 423 K for 24 h. Recently, Tichit et al. [15] have studied the structural and acid–base properties of Mg/Al and Mg/Ga LDH obtained by microwave irradiation of the coprecipitated gels, that were compared with those conventionally aged by prolonged hydrothermal treatment (18 h at room temperature). The authors found that the use of microwaves reduces significantly the duration of the synthesis, and similar crystallinities and chemical composition were obtained whatever the synthesis method used. Interestingly, while the specific surface areas of the mixed oxides obtained by calcinations at 723 K of the LDHs conventionally prepared were higher than the microwave-irradiated ones, microcalorimetric and spectroscopic measurements upon CO_2 and CH_3CN adsorption showed that in the case of Mg/Al mixed oxides, the amount of both basic and acid sites increases when the LDHs is synthesized using microwave irradiation. They conclude that the microwave treatment probably induces higher amounts of surface-defective sites.

From a catalytic point of view, the synthesis of high surface area hydrotalcites, the derived mixed oxides, and their corresponding regenerated hydrotalcites are matters of interest, since this should have an impact on the total number as well as the basic strength of the solid, and on its catalytic activity. Keeping this in mind, several studies show that sonication enhances and/or alters the dissolution process and nucleation and growth of precipitates in some inorganic synthesis [16–18]. Kapustin [19] examined 30 different samples and observed that insonating the solution during crystallization alters the grain size of crystals and produces fine-structured crystals which have smaller grain sizes than the crystals prepared without insonation. Interestingly, we have not found any report on the application of the ultrasound irradiation during the synthesis of hydrotalcites; however, Seida et al. [20] applied sonication after the synthesis of the hydrotalcite. The authors found in this case that the LDHs present larger crystallites and BET surface areas than conventionally prepared samples.

Calcined and calcined rehydrated Mg–Al hydrotalcites have found numerous applications as basic catalysts in organic reactions such as Knoevenagel, Claisen–Schmidt, and aldol condensations, Michael additions, phenol alkylations, or epoxidation of olefins [21]. Thus, for a calcined hydrotalcite with a given chemical composition, the number of basic sites can be controlled by modifying the specific surface area of the solid, whereas the basic strength can be controlled by modifying the number of defects in the framework of the material, i.e., the number of oxygen atoms associated with Mg exhibiting a low coordination number. Although the base strength of calcined hydrotalcites has been considered to be close to superbases [21], in numerous applications where water is produced (for instance, condensation reactions), the presence of water reduces the base strength to moderate levels.

In this work, we have attempted the synthesis of Mg/Al hydrotalcites, the corresponding amorphous mixed oxides, and the rehydrated HT with higher surface areas and smaller crystallite (particle) sizes than the conventional HT, with the aim of increasing both number and base strength of the active sites. In order to achieve this, we undertook the synthesis of three series of LDHs. In two of them, the effect of the temperature during the coprecipitation step, with and without simultaneous sonication, was studied. In the third series we investigated the influence of the temperature during the ageing step of the gels under simultaneous microwave irradiation. The effect of these different synthetic methodologies on the structural and textural properties of the materials and their impact on their catalytic activity for two base-catalyzed organic reactions, i.e., Knoevenagel condensation and aldol condensation, are presented. We have shown that by “in situ” sonication during the synthesis, it is possible to produce samples that, to the best of our knowledge, give the highest catalytic activity reported up to now.

2. Experimental

2.1. Preparation of catalysts

An Mg–Al hydrotalcite with a Mg/Al ratio of 3 was prepared from gels produced by mixing two solutions: solution A containing $(3 - x)$ mol of $Mg(NO_3)_2$ and x mol of $Al(NO_3)_3$ in the Al + Mg concentration of 1.5 mol/L for a ratio $x/3$ of 0.25, and another solution B of $(6 + x)$ mol of NaOH and 2 mol of Na_2CO_3 dissolved in the same volume of the solution A. Both solutions are coadded at a rate of 1 $mL\,min^{-1}$ under vigorous mechanical stirring, at room temperature. The suspension was left for 18 h at 333 K. The hydrotalcite was filtered and washed until pH 7, and the solid was dried at 333 K. The HT was activated by calcining at 723 K in dry nitrogen for 6 h. This mixed oxide is called in the text the HTc_{CV} sample.

The first hydrotalcite series (HT_T) was prepared by coprecipitation at constant and controlled pH, by slow addition in a single container of two diluted solutions (A and B). Solution A contains $Mg(NO_3)_2$ and $Al(NO_3)_3$, of 1.5 M in Al + Mg with Al/(Al + Mg) molar ratio equal to 0.25, and solution B prepared by dissolving Na_2CO_3 and NaOH in water in such way that the ratio ${CO_3}^{2-}/(Al + Mg)$ is equal to 0.66. The solutions were mixed at a 60 $mL\,h^{-1}$ addition rate, for 4 h, with vigorous stirring. The final pH was 12–13. The coaddition process was carried out at different temperatures (298, 313, 333, 353, and 373 K). Finally, the precipitate was filtered, washed to eliminate the alkali metals and the nitrate ions until the pH of the washing water was 7, and then dried at 333 K for 12 h. The samples were not aged and are called HT_{T298}, HT_{T313}, HT_{T333}, HT_{T353}, and HT_{T373}.

The second and third series were prepared by adding the solution containing the Mg^{2+} and Al^{3+} ions (solution A) into one containing Na_2CO_3 or NaOH (solution B).

For the second series the gels obtained were aged into a stainless-steel autoclave placed into a microwave oven (MARS, microwave accelerated reaction system), at different temperatures (313, 353, 393, 433, 473, and 513 K) for 1 h. After the precipitate was filtered and washed until pH 7, the solid was dried at 333 K for 12 h. The samples were labeled as HT_{MW313}, HT_{MW353}, HT_{MW393}, etc.

The preparation of the third series was carried out as described above, but adding an aqueous solution (A) containing the metal cations (Mg^{2+} and Al^{3+}) onto a solution containing the base (B) with simultaneous ultrasound irradiation of the mixture (SIC Vibracell VCX400). This procedure was carried out at atmospheric pressure and at different temperatures: 273, 283, 298, and 323 K. The gels obtained were not aged. These samples were labeled as HT_{US273}, HT_{US283}, etc. Finally, the precipitate was filtered, washed to eliminate the alkali metals and the nitrate ions until the pH 7, and then dried at 333 K for 12 h.

The hydrotalcites were calcined at 723 K for 6 h in a nitrogen flow, in order to obtain Mg–Al mixed oxide base catalysts. Samples of the mixed oxides were rehydrated at room temperature by direct decarbonated water (MilliQ) addition just before their use as catalysts.

Specific surface areas of the different hydrotalcites were obtained with an ASAP 2000 (Micromeritics) using the BET methodology. The samples were pretreated at 673 K prior to N_2 adsorption. The solids were characterized by X-ray diffraction (XRD) with a Phillips PW diffractometer using Cu-K_α radiation. Sonic energy was provided by an ultrasonicator (SIC Vibracell VCX400) which generates 20 kHz ± 50 Hz ultrasound waves. Microwave irradiation was performed in a conventional oven (300 W).

A scanning electron microscope (JEOL6300) equipped with a microanalysis system by disperse energy (Oxford Instruments Link-ISIS) was used to obtain SEM images.

2.2. Catalytic activity

2.2.1. Reaction procedure

A commercial citral sample formed by a mixture of *cis* and *trans* isomers (geranial and neral) with a proportion of 25 and 75% (wt/wt), respectively, was used without further purification. Acetone, malononitrile, benzaldehyde, and ethyl cyanoacetate were purchased from Aldrich and used directly.

2.2.2. Aldol condensation of citral with acetone

Typically, a mixture of citral (6.5 mmol), acetone (18.2 mmol), and catalyst (414 mg, 16.6% (wt/wt)) were added in a three-necked bottom flask equipped with a condenser system. The resultant suspension was heated up to 333 K under vigorous stirring in an oil bath equipped with an automatic temperature control system. Samples were taken at regular time periods and analyzed by gas chromatography (GC) with a flame ionization detector and a Tracer wax capillary column (15 m × 0.32 mm × 0.25 µm). At the end of the reaction, after cooling, the reaction mixture was filtered to remove the catalyst and analyzed by GC.

2.2.3. Knoevenagel condensation between benzaldehyde and malononitrile

A mixture of benzaldehyde (10 mmol) and malononitrile (10 mmol) at 298 K, under an inert atmosphere (N_2), was magnetically stirred, and calcined hydrotalcite (2.7% (wt/wt)) was added. Samples were taken periodically during the reaction, within a time period of 0.1 to 2 h, and analyzed by GC with a flame ionization detector and a HP-5 capillary column (30 m × 0.32 mm × 0.25 µm).

2.2.4. Knoevenagel condensation between benzaldehyde and ethyl cyanoacetate

A mixture of benzaldehyde (10 mmol) and ethyl cyanoacetate (10 mmol) under an inert atmosphere (N_2) was placed in a flask which was immersed in a thermostat silicone oil bath at 333 K and magnetically stirred. Then, the calcined hydrotalcite (5.5% (wt/wt)) was added. Samples of the reaction mixture were periodically taken with a time period of 0.1 to 2 h and analyzed by GC with a flame ionization detector and a HP-5 capillary column (30 m × 0.32 mm × 0.25 µm).

In all experiments, nitrobenzene was used as internal standard. At the end of the reaction, after cooling, the reaction mixture was filtered to remove the catalyst and analyzed. Each reaction product was identified by GC-MS (Hewlett-Packard 5988 A) and by ^{1}H NMR spectroscopy (Varian VXR-400S, 400 MHz).

It was found that for particle sizes below 0.3 mm diameter, the reaction is not controlled by diffusion.

3. Results and discussion

3.1. Characterization of materials

The results of the XRD measurements obtained for the three series HT_T, HT_{MW}, and HT_{US} are presented in Figs. 1, 2, and 3, respectively. The XRD patterns of the prepared LDH present sharp and symmetric peaks for (003), (006), (110), and (113) planes, as well as broad symmetric peaks for the (009), (015), and (016) planes. These peaks are characteristics of clay minerals having layered structures

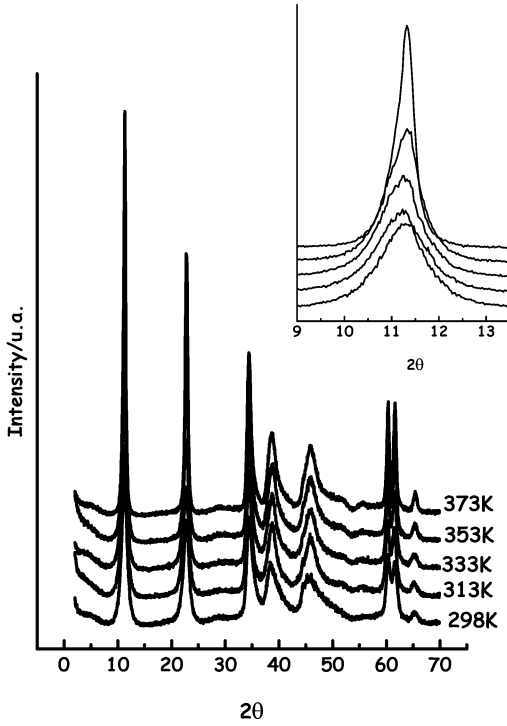

Fig. 1. $\mathrm{HT_T}$ series. Effect of the temperature during the coprecipitation step on the intensities XRD reflections.

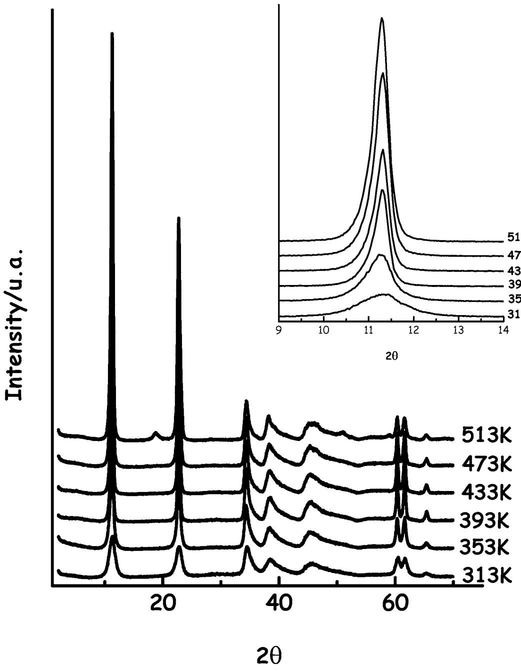

Fig. 2. $\mathrm{HT_{MW}}$ series. Effect of the temperature during the ageing step on the intensities XRD reflections.

[22,23], and they show that in all cases, well-crystallized hydrotalcites are formed.

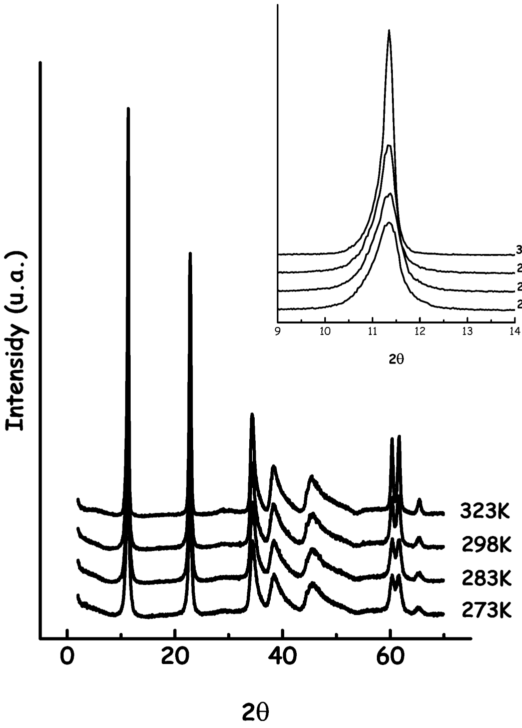

Fig. 3. $\mathrm{HT_{US}}$ series effect of the temperature during the ageing step on the intensities XRD reflections.

Table 1
Crystallite size of the samples measured from XRD using the Debye–Sherrer equation

Sample	Crystal size, Å Plane (003)	Crystal size, Å Plane (110)	Crystal size, Å Plane (113)
$\mathrm{HT_{CV}}$	200	310	235
$\mathrm{HT_{T298}}$	80	127	103
$\mathrm{HT_{T313}}$	79	138	108
$\mathrm{HT_{T333}}$	93	165	119
$\mathrm{HT_{T353}}$	120	214	159
$\mathrm{HT_{T373}}$	120	246	213
$\mathrm{HT_{MW313}}$	85	131	120
$\mathrm{HT_{MW353}}$	152	255	209
$\mathrm{HT_{MW393}}$	395	497	415
$\mathrm{HT_{MW433}}$	403	510	592
$\mathrm{HT_{MW473}}$	414	423	310
$\mathrm{HT_{MW513}}$	431	338	235
$\mathrm{HT_{US273}}$	163	115	103
$\mathrm{HT_{US283}}$	179	122	120
$\mathrm{HT_{US298}}$	166	162	155
$\mathrm{HT_{US323}}$	390	314	282

Crystal sizes of the different synthesized hydrotalcites.

From Figs. 1, 2, and 3 we can see that the intensity of the peaks increases when increasing the synthesis temperature, which can be correlated with an increase of the crystallinity of the samples. To corroborate this observation, the crystallite size of the samples was measured from the X-ray line broadening, considering the basal reflections (003), (110), and (113), and using the Debye–Sherrer equation. The results are summarized in Table 1. As can be seen there, an increase of the crystal size occurs when increasing the temperature, regardless of the synthesis method. This indicates that increasing the temperature during the coprecipitation or during the ageing step, causes the rate of nucleation to be lower than the rate of crystal growth.

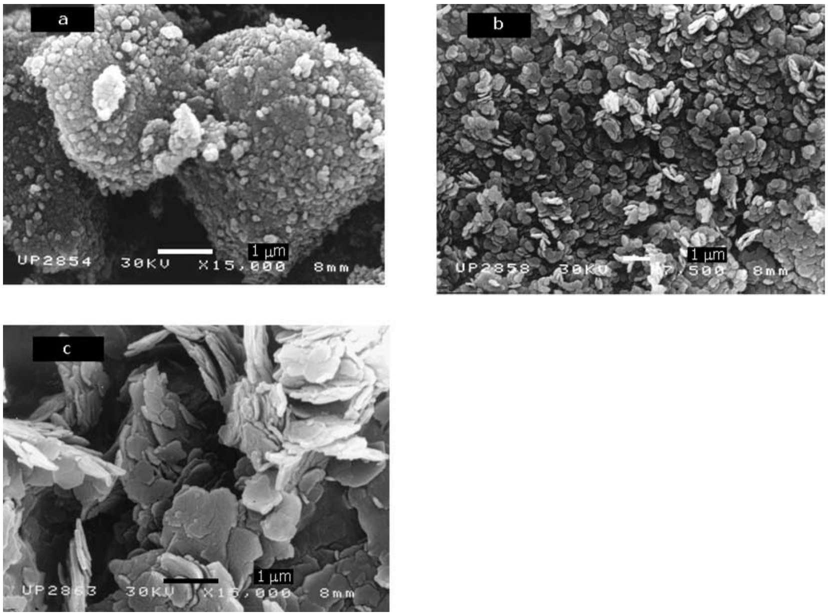

Fig. 4. SEM images for HT_{MW353} (a); HT_{MW433} (b); HT_{MW513} (c).

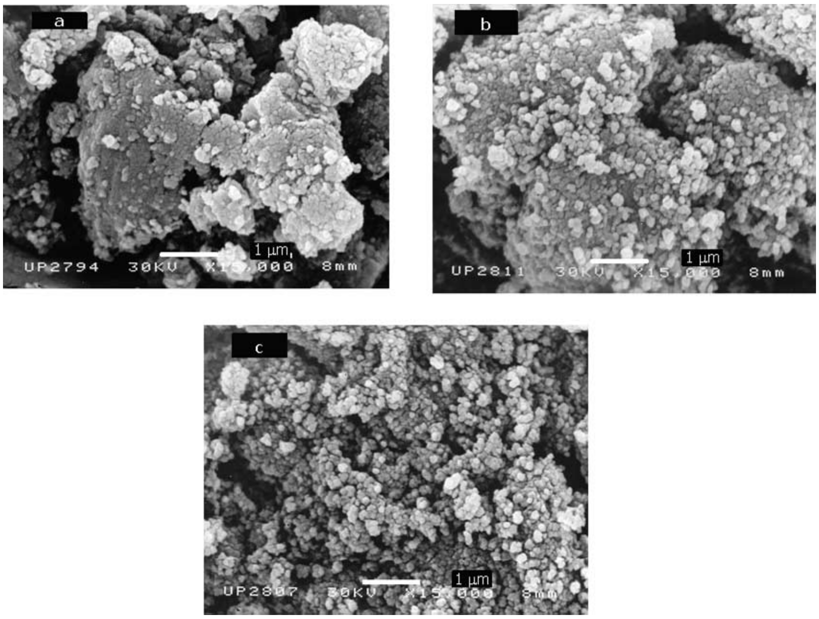

Fig. 5. SEM images of the samples HT_{CV} (a); HT_{T353} (b); HT_{US298} (c).

In order to determine the morphology and particle size distribution of the LDH of these series, we have selected different representative samples which where studied by scanning electron microscopy (SEM). In Fig. 4, the SEM micrographs of three samples pertaining to the series HT_{MW}, which where aged at different temperatures in a microwave oven, are displayed. As Fig. 4 shows, the particle size increases when increasing the temperature, with average sizes of 120, 320, and 540 nm for samples HT_{MW353}, HT_{MW433} and HT_{MW513}, respectively.

In Fig. 5 the SEM images for samples of the series HT_T and HT_{US}, which were not submitted to the ageing process, are presented and compared with the sample (HT_{CV}) synthesized following the conventional procedure. The microphotographs show that HT_{T353} and HT_{CV} present similar morphologies, with an average particle sizes in the range of 100–120 nm, which are similar to those displayed by the sample HT_{MW353} (Fig. 4a). However, the sample prepared under sonication at 298 K (Fig. 5c), presents an extremely homogeneous morphology and highly dispersed particles with an average size of 80 nm.

The three LDHs series were calcined at 723 K in order to obtain the corresponding Mg–Al mixed oxides. The specific surface areas of the calcined samples (HTc) were measured

Table 2
Surface properties of HTc$_{T}$ series

Sample	S_{BET} ($m^2\ g^{-1}$)	S_{MIC}[a] ($m^2\ g^{-1}$)	Pore volume ($cm^3\ g^{-1}$)	Micropore volume[a] ($cm^3\ g^{-1}$)	Pore diameter (Å)
HTc$_{CV}$	245	20	0.62	0.062	94.7
HTc$_{T298}$	264	127	0.40	0.017	72.9
HTc$_{T313}$	272	46	0.91	0.021	133.6
HTc$_{T333}$	268	83	0.77	0.038	116.0
HTc$_{T353}$	265	77	0.82	0.038	128.0
HTc$_{T373}$	264	161	0.59	0.074	0.59

Results of adsorption/desorption of nitrogen of different calcined hydrotalcites samples (HTc$_{T}$ series).

[a] Microporous area calculated from the t plot, using as reference t, between 5.5 and 8.5.

Table 3
Surface properties of HTc$_{MW}$ series

Sample	S_{BET} ($m^2\ g^{-1}$)	S_{MIC}[a] ($m^2\ g^{-1}$)	Pore volume ($cm^3\ g^{-1}$)	Micropore volume[a] ($cm^3\ g^{-1}$)	Pore diameter (Å)
HTc$_{CV}$	245	20	0.62	0.062	94.7
HTc$_{MW313}$	270	45	0.27	0.023	85.60
HTc$_{MW353}$	277	56	0.61	0.024	89.76
HTc$_{MW393}$	251	170	0.49	0.080	82.23
HTc$_{MW433}$	246	176	0.41	0.085	68.74
HTc$_{MW473}$	246	175	0.39	0.087	66.54
HTc$_{MW513}$	237	162	0.363	0.082	63.31

Results of adsorption and desorption of nitrogen of different calcined hydrotalcites samples (HTc$_{MW}$ series).

[a] Microporous area calculated from the t plot, using as reference t, between 5.5 and 8.5.

by N_2 adsorption at 77 K. The results are summarized in Table 2 for the HTc$_{T}$ series, and they are compared with those of a sample synthesized by a conventional procedure (HTc$_{CV}$). As we can observe, all samples of the HTc$_{T}$ series exhibit very similar specific surface areas, indicating that in the range studied, the variation of temperature during the coprecipitation step has no influence on the BET surface area of the mixed oxide, despite the fact that the crystal size of the LDH precursor increases with increasing synthesis temperature (Fig. 1 and Table 1). However, when these results are compared with the mixed oxide from a sample obtained by the conventional method (HTc$_{CV}$), we can observe that the HTc$_{CV}$ sample has a lower specific surface area and lower porosity than the samples of the HTc$_{T}$ series. It should be taken into account that, the HTc$_{CV}$ sample was submitted, after coprecipitation, to an ageing time of 18 h at 333 K, which favors the crystallization process and produces a decrease of the surface area of the mixed oxide obtained by calcination.

In Table 3 the results of the BET surface areas for the mixed oxides produced by calcination of samples of the HT$_{MW}$ series are presented. In this series, the gels were aged in a microwave oven at different temperatures for 1 h, and one can observe that an increase of the temperature produces a decrease in the BET area, along with an increase of the microporosity. This result can be attributed to the crystallinity increase of the LDHs precursor with temperature (Fig. 2), that is accompanied by an increase of the crystal size. When these results are compared with those obtained for the series HTc$_{T}$ (Table 2) and with the conventional sample (HTc$_{CV}$), we can conclude that the ageing treatment under microwave irradiation at temperatures lower than 393 K allows mixed oxides with higher specific surface areas to be produced.

The results presented above in Table 2, showed that during the coprecipitation step, the temperature has no influence on the final specific surface areas of the mixed oxides produced by calcination (HTc$_{T}$ series). However, different results were obtained for the calcined samples when the gels were submitted during precipitation to ultrasounds irradiation (Table 4). Although the results of Table 4 do no show a clear tendency for the variation of the BET area with temperature, it is clear that the sample which is synthesized at 298 K (HTc$_{US298}$) under sonication presents a surface area 20% larger than that of the conventionally synthesized sample and any of the series HTc$_{T}$ and HTc$_{MW}$. It is known that when a liquid–solid interface is submitted to ultrasounds, acoustic cavitations [24] near the surface induce markedly asymmetric bubble collapse, which generates a high-speed jet of liquid directed at the surface [25]. The collision of this jet and related shock waves can create a localized erosion on the surface (which can produce defective sites), improve mass transport, and can cause particle fragmentation (which can increase the surface area) [26]. Taking into account that the crystallization process starts since the beginning of the coprecipitation step, these results suggest that ultrasounds, not only accelerate the crystal formation, as it has been previously observed [20], but they can also cause the dispersion of small groups of layers of the LDH as well as reducing agglomeration during the nucleation and crystal growing process, giving rise to particles with small crystal sizes. Such

Table 4
Surface properties of HTc_{US} series

Sample	S_{BET} ($m^2 g^{-1}$)	S_{MIC}[a] ($m^2 g^{-1}$)	Pore volume ($cm^3 g^{-1}$)	Micropore volume[a] ($cm^3 g^{-1}$)	Pore diameter (Å)
HTc_{CV}	245	20	0.62	0.062	94.7
HTc_{US273}	275	77	0.715	0.32	103.77
HTc_{US283}	263	88	0.629	0.04	95.36
HTc_{US298}	284	138	0.607	0.04	96.75
HTc_{US323}	254	62	0.624	0.01	98.20

Results of adsorption and desorption of nitrogen of different calcined hydrotalcites samples (HTc_{US} series).

[a] Microporous area calculated from the t plot, using as reference t, between 5.5 and 8.5.

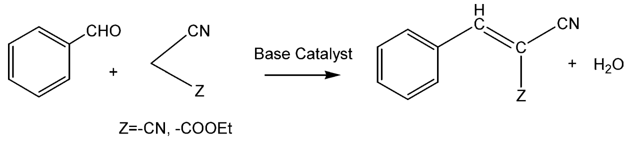

Scheme 1.

effects will not only increase the surface area of the mixed oxide derivative, but it will also increase the structural defects of the solid. This possibility will be tested below by catalytic activity measurements.

3.2. *Catalytic activity*

In order to check the influence of the preparation method of the layered material on the catalytic activity of the mixed oxides obtained by calcination, we selected different samples of HTc pertaining to the three different series: HTc_{T353}, HTc_{MW433}, HTc_{US273}, and HTc_{US298}. These materials were tested as basic catalysts for the Knoevenagel condensation and aldol condensation between citral and acetone.

3.2.1. *Knoevenagel condensation*

Knoevenagel condensation [27] of carbonyl compounds with reactants containing an active methylenic group is one of the most important methods for preparating substituted alkene derivatives (Scheme 1). These compounds are of interest as end products and intermediates in the production of fine chemicals and commodities such as perfumes [28], pharmaceuticals [29], and polymers [30]. Besides the importance of the Knoevenagel condensation as a synthetic organic method, another relevant characteristic of this reaction is its ability to measure the total number of basic sites and the relative strength of different base catalysts, by reacting a series of methylenic compounds with different pK_a values [31]. Then, the different mixed oxides were tested for the Knoevenagel condensations between benzaldehyde and malononitrile (MN) ($pK_a = 11$) or ethyl cyanoacetate (ECA) ($pK_a = 9$) (Scheme 1). It should be pointed out, that according to the pK_a's reported in the literature and which were determined in aqueous solutions, the decreasing order of acidity of the reactants is ECA > MN. However, calculations of the positive charge density of the hydrogen at the methylenic groups give us values of 0.34 and 0.32 for malononitrile and ethyl cyanoacetate, respectively, indicating that the order of acidity is MN > ECA.

The selected calcined HTc samples (HTc_{T353}, HTc_{MW433}, HTc_{US273}, and HTc_{US298}) were tested for the Knoevenagel condensation between benzaldehyde and MN, (molar ratio 1:1) using a 2.7% (wt/wt) of catalyst with respect to the total amount of reagents, at 298 K and without solvent. The results of initial activity (initial reaction rate, determined at a low level of conversion, i.e., $x < 10\%$) as well as the yield to the Knoevenagel adduct (**1**) are presented in Table 5. There, they are compared with the results obtained with a mixed Mg–Al oxide synthesized by the conventional methodology. In all cases, the selectivity to the Knoevenagel condensation compound was of 100%, and no product coming from Michael addition of the MN to the Knoevenagel adduct was observed. As it is displayed in Table 5 the order of activity was: $HTc_{US298} > HTc_{US273} > HTc_{T353} > HTc_{MW433} > HTc_{CV}$. In Fig. 6 the activity of the catalysts per unit surface area is plotted versus the BET surface area of the samples.

For the condensation of benzaldehyde and ECA, the reactions were carried out using a 5.5% (wt/wt) of catalysts at 333 K. In this case the selectivity for the Knoevenagel product (**2**) was also 100%, and the same order of activity (Table 6) and activity per unit surface area (Fig. 6) were observed.

The results show that the specific catalyst activity increases when increasing the surface area of the mixed oxides, and it is maximum for the mixed oxide produced from the hydrotalcite obtained by in situ sonication during precipitation (Tables 5 and 6). These results clearly show that, as can be expected, the total number of basic sites increases when increasing the surface area of the solid. However, results from Fig. 6 also show that the activity increase with surface area is not lineal but exponential. This indicates that by increasing the surface area, i.e., decreasing the "crystal size" of the mixed oxide, active sites with different strengths should be produced.

In the case of Mg–Al mixed oxides formed by the controlled calcinations of hydrotalcites, the active basic sites are associated to hydroxide groups and different of O^{-2}–Mg^{2+} acid–base pairs [4]. The basicity of the Lewis sites associated to O^{-2} anions depends on their coordination. Those

Table 5
Results of the Knoevenagel condensation between benzaldehyde and malononitrile

Sample	S_{BET} ($m^2\ g^{-1}$)	$r_0 \times 10^3$ ($mol\ g^{-1}\ min^{-1}$)	$r_0/S \times 10^6$	Yield **1**, 15 min (%)	Yield **1**, 240 min (%)
HTc_{CV}	245	1.950	8.0	23	95
HTc_{T353}	265	2.437	9.2	38	96
HTc_{MW433}	246	2.083	8.4	32	82
HTc_{US273}	275	3.413	12.4	44	83
HTc_{US298}	284	3.812	13.4	50	91

Condensation of benzaldehyde with malononitrile in the presence of different calcined hydrotalcites.

Table 6
Results of the Knoevenagel condensation between benzaldehyde and ethyl cyanoacetate

Sample	S_{BET} ($m^2\ g^{-1}$)	$r_0 \times 10^3$ ($mol\ g^{-1}\ min^{-1}$)	$r_0/S \times 10^6$	Yield **2**, 5 min (%)	Yield **2**, 240 min (%)
HTc_{CV}	245	4.457	18.2	31	88
HTc_{T353}	265	5.986	22.6	42	91
HTc_{MW433}	246	4.343	17.7	30	91
HTc_{US273}	275	6.943	25.2	49	93
HTc_{US298}	284	8.514	30.0	60	96

Results of the Knoevenagel condensation between benzaldehyde and ethyl cyanoacetate in the presence of different calcined hydrotalcites.

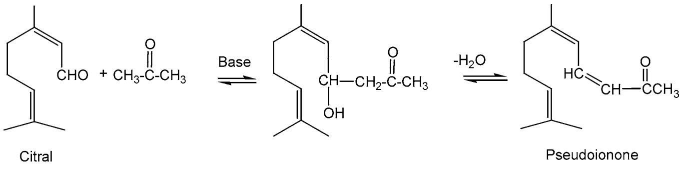

Scheme 2.

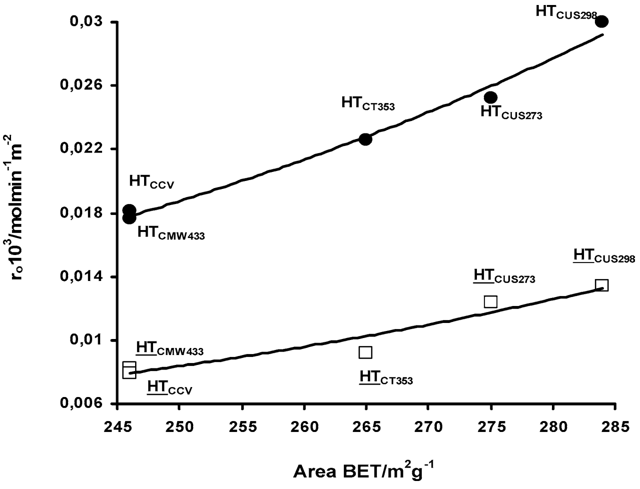

Fig. 6. Influence of the area BET on the initial formation rate of **1** (□) and **2** (●).

oxygen atoms located in corners of the crystal should have a stronger basicity than oxygen atoms located either on edges or on crystal faces [32]. Then, we have to expect that samples with lower "crystal size" possess higher concentrations of Lewis sites of low coordination number, and therefore the basicity should be higher. Since in our samples, the specific activity increases when increasing the surface area, we have to conclude that an increase of surface area not only leads to an increase of the number of active sites, but also increases the fraction of the stronger ones which is maximum for samples synthesized by the sonication treatment.

3.2.2. *Citral–acetone condensation*

In order to check our hypothesis we selected a more demanding reaction from the point of view of basic strength: the aldol condensation between citral and acetone (Scheme 2). In fact, for carbonylic compounds, the pK_a associated with the hydrogen at the methyl and methylene groups in the alpha position to the carbonyl group is in the range of 25. Particularly for the acetone, the positive charge density of the hydrogen at the methyl group was +0.12, which is a value considerably lower than that of the methylene-active compounds tested previously in the Knoevenagel condensation (+0.34 and +0.32). Moreover, this reaction has industrial interest because it produces ionones (cyclic terpenoids), which are used for enhancing the organoleptic properties of consumables such as medicinal products and fragrances and as intermediates in vitamin A synthesis.

Although this condensation reaction can be catalyzed by either acid or bases, numerous commercial methods make use of conventional homogeneous bases as catalysts (i.e., aqueous alkali metal hydroxide solutions, alcoholates in alcohol, or benzene solvents) which lead to waste streams. However, owing to the industrial importance of the process, solid catalysts such as basic alumina, alkali oxides, MgO,

Table 7
Results of the aldol condensation of citral with acetone

Sample	S_{BET} ($m^2\ g^{-1}$)	$r_0 \times 10^3$ ($mol\ g^{-1}\ min^{-1}$)	$r_0/S \times 10^6$	Yield **3**[a] (%)	Selectivity **3**[a] (%)
HTc_{CV}	245	0.42	1.7	68	82
HTc_{T353}	265	0.58	2.2	81	83
HTc_{MW433}	246	0.39	1.6	64	86
HTc_{MW513}	237	0.38	1.6	61	87
HTc_{US273}	275	0.58	2.1	78	88
HTc_{US298}	284	0.74	2.6	93	95

Results of the aldol condensation between citral and acetone using different synthesized calcined hydrotalcites.

[a] At 1 h reaction time.

and calcined hydrotalcites may have an opportunity as potential industrial catalysts.

In previous work [33], we have studied the aldol condensation between citral and acetone in the presence of Mg–Al calcined hydrotalcites at 333 K, and we have found that it is possible to obtain excellent conversions and selectivities to pseudoionones working with relatively low acetone to citral molar ratios. Thus, when the aldolic condensation between citral an acetone was carried out in the presence of the calcined hydrotalcites described in this work (16.6% (wt/wt)), at 333 K using a molar ratio acetone/citral of 2.8, the main products obtained were a mixture of *cis* and *trans* pseudoionones (**3**) (6,10-dimethyl-3,5,9-undecatrien-2-one) (Scheme 2). Besides, the pseudoionones, other condensation products coming from the self-condensation of acetone, self-condensation of citral, and oligomers derived from citral were detected in the reaction mixture. No β-hydroxyl ketones derived from acetone or pseudoionones were detected under these experimental conditions.

In Table 7 yields and selectivities to pseudoionones obtained with the selected calcined HTc samples (HTc_{T353}, HTc_{MW433}, HTc_{MW513}, HTc_{US273}, and HTc_{US298}) and mixed Mg–Al oxide synthesized by the conventional methodology (HTc_{CV}) after a 1 h reaction time are summarized. Results from Table 7 clearly indicate that the HTc_{US298} gives a larger catalytic activity than HTc_{CV} or any other of the calcined hydrotalcites, with the order of activity $HTc_{US298} > HTc_{US273} = HTc_{T353} > HTc_{MW433} > HTc_{CV} > HTc_{MW513}$.

When the specific activity for pseudoionone formation was plotted versus the specific surface area of different mixed oxides (Fig. 7) it was possible to see that, as it was observed previously for Knoevenagel condensation, an increase of the surface area of the calcined hydrotalcites does not only increase the number of basic sites, but also the fraction of the stronger ones. Furthermore it appears that the mixed oxide obtained from the hydrotalcite synthesized by applying ultrasounds is almost twice more active than the hydrotalcite prepared by a conventional procedure. Indeed, it was possible with the HTC_{US298} catalyst to obtain after 1 h reaction time a yield of pseudoionones of 93%, with a selectivity of 95%. On the other hand in the presence of HTc_{CV} only a yield of 68% with selectivity of 82% was found.

It must be noted that XRD of the mixed oxides performed after their use as catalysts for the Knoevenagel and aldol condensations showed that hydrotalcite was not regenerated during the reaction.

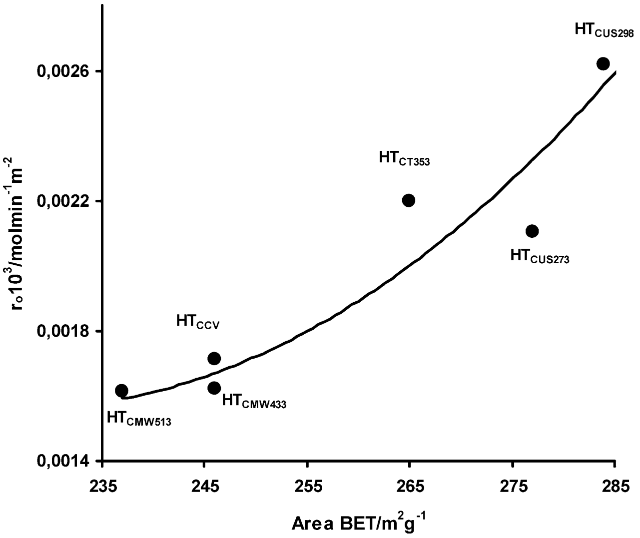

Fig. 7. Influence of the area BET of different calcined hydrotalcite samples on the initial rate of formation of pseudoionones **3**.

3.3. Hydrotalcites regenerated by rehydration

Recently, it has been presented that a calcined hydrotalcite can be activated by rehydration at room temperature by contacting with a stream of nitrogen saturated with water vapor, during long periods of time or by directly adding water to the calcined solid [34,35].

It is a general belief that the basic sites produced by calcination are oxygen anions of low coordination, which correspond to Lewis basic sites. However when the calcined hydrotalcite is rehydrated, basic Lewis sites are converted to basic hydroxyl Brønsted sites, which become the compensating interlayer anions. On the other hand, it has been presented in the literature that rehydrated mixed oxides were very active for aldol condensation reactions such as the self-condensation of acetone [36], condensation of benzaldehyde with acetone [37], condensation of citral, with acetone or methyl ethyl ketone, and the Claisen–Schmidt condensation [38].

It is known that the aldol condensation is a reversible reaction when water is one of the products, and an excess of

Table 8
Results of aldol condensation between citral and acetone in the presence of hydrotalcite sample (HTc_{US298}) using different percentages of water added

Water added (%)	$r_0 \times 10^3$ ($\mathrm{mol\,g^{-1}\,min^{-1}}$)	Yield **3**, 15 min (%)	Selectivity **3** (%)
0	0.71	69	88
20	0.87	83	97
36	1.00	96	99
46	0.88	84	98

Reaction conditions: acetone (18.2 mmol), citral (6.5 mmol), 414 mg of catalyst, at 333 K.

water on hydrotalcite should shift the reaction equilibrium toward the formation of the reactants. According to this, the condensation reaction between citral and acetone was performed adding on the calcined hydrotalcite (HTc_{US298}) at different percentages of water with respect to the solid catalyst (20, 36, and 46% (wt/wt)). In Table 8 it can be seen that the calcined hydrotalcite was less active than the rehydrated samples and a maximum of activity was found when the condensation was carried out using freshly calcined hydrotalcite with 36% (wt/wt) of water added of. It is very interesting to note, that the optimized rehydrated sample reached yields of pseudoionones of 96% with 99% of selectivity in 15 min of reaction time, working at a very low acetone/citral molar ratio. This result is superior to any reported up to now for this condensation in a homogeneous and heterogeneous phase.

4. Conclusions

It has been shown that during the synthesis of Mg–Al LDH, the increase of temperature during the coprecipitation step with and without simultaneous sonication (HT_T and HT_{US} series, respectively) or during the ageing step of the gels under microwave irradiation (HT_{MW} series) causes an increase of the crystal size.

It has been found that the sample prepared under sonication at 298 K (HT_{US298}) compared with samples of other series presents a homogeneous morphology and highly dispersed particles with an average size of 80 nm. The larger surface area presented by the mixed oxide derivative (HTc_{US298}) (20% larger than that of the mixed oxide conventionally synthesized) not only could be due to the fact that ultrasounds accelerate the crystal formation, but also to the dispersion of small groups of layers and decreasing agglomeration during the nucleation and crystal growing process, affording crystals with smaller sizes than those obtained by a conventional ageing method. We have shown that mixed oxides derived from hydrotalcites synthesized by using ultrasound have improved considerably the surface area of the calcined hydrotalcite, as well as the number of the accessible active sites.

The corresponding mixed oxides obtained by calcination of the hydrotalcites prepared with ultrasound present a higher specific activity for Knoevenagel and aldol condensations. This was explained by assuming that the increase in surface area, not only changes the total number of the basic sites exposed to reactants, but also increases the fraction of the stronger ones. These correspond to O^{2-} located in corners of the crystals. Then, the smaller the crystal size the larger the fraction of the above sites, and the larger the total number of the exposed sites. This agrees very well with the fact the regenerated hydrotalcites show a larger amount of accessible Brønsted basic sites for samples with a higher surface area. Using this rehydrated material it is possible to obtain yields of pseudoionones of 96% with 99% of selectivity, in 15 min of reaction time working at a very low acetone/citral molar ratio. This result is superior to any reported up to now for this condensation in homogeneous and heterogeneous phases.

Acknowledgment

Financial support of the Spanish Ministry of Science and Technology (MAT2003-079-45-CO2-01) is acknowledged.

References

[1] F. Cavani, F. Trifiro, A. Vaccari, Catal. Today 11 (1991) 173.
[2] R. Allmann, Chimia 24 (1970) 99.
[3] S. Miyata, Clays Clay Miner. 28 (1980) 50.
[4] W.T. Reichle, S.Y. Kang, D.S. Everhardt, J. Catal. 101 (1986) 352.
[5] H.F.W. Taylor, Miner. Mag. 37 (1969) 338.
[6] J. Valente, F. Figueras, M. Gravelle, P. Kumbhar, L. Lopez, J.P. Besse, J. Catal. 189 (2000) 370.
[7] D. Tichit, M.H. Lhouty, A. Guida, B.H. Chiche, F. Figueras, A. Aroux, D. Bartalini, E. Garrone, J. Catal. 151 (1995) 50.
[8] D.M.P. Mingos, D.R. Baghurst, Chem. Soc. Rev. 20 (1991) 1.
[9] S. Komarneni, R. Roy, Q.H. Li, Mater. Res. Bull. 27 (1992) 1393.
[10] S. Komarneni, R. Roy, Q.H. Li, J. Mater. Chem. 4 (1994) 1903.
[11] S. Komarneni, R. Roy, Q.H. Li, J. Mater. Res. 11 (1996) 1866.
[12] S. Möhmel, I. Kurzawski, D. Uecker, D. Müller, W. Gebner, Cryst. Res. Technol. 37 (2002) 359.
[13] S. Kannan, R.V. Jasra, J. Mater. Chem. 10 (10) (2000) 2311.
[14] G. Fetter, F. Hernández, A.M. Maubert, V.H. Lara, P. Bosch, J. Porous Mat. 4 (1997) 27;
G. Fetter, P. Bosch, F.A. Hernandez, Mater. Res. Soc. Symp. Proc. 454 (1997) 235.
[15] D. Tichit, A. Rolland, F. Prinetto, G. Fetter, M.J. Martinez-Ortiz, M.A. Valenzuela, P. Bosch, J. Mater. Chem. 12 (2002) 3832.
[16] Y. Fang, D.K. Agrawal, D.M. Roy, P.W. Brown, J. Mater. Res. 7 (1992) 2294.
[17] J.S. Hu, K.K. Agrawa, Y. Fang, R. Roy, J. Mater. Sci. 28 (1993) 5297.
[18] N. Enomoto, H.L. Choi, M. Katsumoto, Z. Nakagawa, Trans. Mater. Res. Soc. Jpn. 14A (1994) 777.
[19] A.P. Kapustin, in: Effect of Ultrasounds on the Kinetics of Crystallization, Consultants Bureau, New York, 1963, p. 65.
[20] Y. Seida, Y. Nakano, Y. Nakamura, Clays Clay Miner. 50 (2002) 525.
[21] B.F. Sels, D.E. De Vos, P.A. Jacobs, Catal. Rev. 43 (2001) 443.
[22] JCPDS X-ray Powder Diffraction File No. 22-700, 1986.
[23] F. Rey, V. Fornes, J.M. Rojo, J. Chem. Soc., Faraday Trans. 88 (1992) 2233.
[24] (a) K.S. Suslick, Adv. Organomet. Chem. 25 (1986) 73;
(b) K.S. Suslick, Modern Synth. Methods 4 (1986) 1.
[25] W. Lauterborn, W. Hentschel, Ultrasonics 24 (1985) 59.
[26] K.S. Suslick, D.J. Casadonte, M.L.H. Green, M. Thompson, Ultrasonics 25 (1987) 56.

[27] L. Knoevenagel, Bersenges 31 (1898) 259.

[28] (a) B. Siebenhaar, WO9721659 (1997);
(b) R.T. Hopp Thielmann, W. Gottsch, US5212153 (1992);
(c) G. Lauterbach, R. Becker, K. Jansen, EP 0395982 (1990);
(d) B. Siebenhaar, B. Casagrande, EP0870750 (1998);
(e) K. Manfred, A. Slagmulder, US4755615 (1988).

[29] (a) M.F. Gordeev, D.V. Patel, WO 9633972 (1996);
(b) E. Castelli, G. Cascio, E. Manghisi, WO9807698 (1998);
(c) A.J. Kesel, W. Oberthür, WO 9820013 (1998).

[30] (a) J.P. Ferraris, T.L. Lambert, S. Rodriguez, WO 9305077 (1993);
(b) R. Schipfer, G. Schmolzer, US 4523007 (1985) and US 4544715 (1985).

[31] A. Corma, V. Fornés, R.M. Martín Aranda, H. Garcia, J. Primo, Appl. Catal. 59 (1990) 237.

[32] E. Garrone, F.S. Stone, in: 8th Int. Cong. Catal., Chemie III, Berlin, 1984, p. 441.

[33] M.J. Climent, A. Corma, S. Iborra, A. Velty, Catal. Lett. 79 (2002).

[34] M.J. Climent, A. Corma, S. Iborra, A. Velty, Green Chem. 4 (2002) 474.

[35] K.K. Rao, M. Gravelle, J. Valente, F. Figueras, J. Catal. 173 (1998) 115.

[36] R. Teissier, D. Tichit, F. Figueras, J. Kervennal, FP 95 00094 (1995).

[37] A. Guida, M.H. Lhouty, D. Tichit, F. Figueras, P. Geneste, Appl. Catal. 164 (1997) 251.

[38] (a) M.J. Climent, A. Corma, S. Iborra, A. Velty, J. Catal. 221 (2004) 474;
(b) J.C.A. Roelofs, D.J. Lensveld, A.J. Van Dillen, K.P. De Jong, J. Catal. 203 (2001) 184.